Targeted Observations of Tropical Cyclones Based on the Adjoint-Derived Sensitivity Steering Vector

Chun-Chieh Wu*, Po-Hsiung Lin, Jan-Huey Chen, and Kun-Hsuan Chou
Department of Atmospheric Sciences
National Taiwan University, Taipei, Taiwan

Abstract

A new way to identify the sensitive area for the targeting of observations for tropical cyclone prediction based on the adjoint model has been proposed in this paper. By appropriately defining the response functions to represent the background steering flow of the tropical cyclone at the verifying time, a simple vector, the Adjoint-Derived Sensitivity Steering Vector (ADSSV), has been designed to clearly demonstrate the sensitivity locations at the observing time. The ADSSV will be implemented and examined in the field project, Dropwindsonde Observations for Typhoon Surveillance near the Taiwan Region (DOTSTAR), as well as the hurricane surveillance program by Hurricane Research Division on the Atlantic in 2005.

Key words：DOTSTAR, targeted of observation

1. Introduction

Since 2003, a field program has been conducted under the name of Dropwindsonde Observations for Typhoon Surveillance near the Taiwan Region (DOTSTAR) (Wu et al. 2005). For DOTSTAR, targeting of observations is one of the most critical objectives. The important basis to formulate the observing strategy is to identify the sensitive areas, which would have critical impact on the numerical forecast results or the rapid growth of the forecast error. Up to the present, three sensitivity products have been used to decide the observing strategy in DOTSTAR. These products are derived from three different techniques. First, the Deep-Layer Mean (DLM) winds variance, which is the variance of the deep-layer steering flow based on the NCEP (National Centers for Environmental Predictions) EFS (Global Ensemble Forecasting System) (Aberson et al. 2003), where areas with the largest forecast deep-layer-mean wind bred vectors indicate the sensitive region at the observing time. Second, the Ensemble-Transform Kalman-filter (ETKF, Bishop and Majumdar 2001), which predicts the reduction in forecast error variance for feasible deployment of targeted observations based, in this cases, on the 40-member NCEP EFS. Third, the Singular Vector (SV) technique (e.g., Palmer et al. 1998) which maximizes the growth of a total energy or kinetic energy norm using, in this case, the forward and adjoint tangent models of the Navy Operational Global Atmospheric Prediction System (NOGAPS, Rosmond 1997; Gelaro et al. 2002).

As mentioned above, the ETKF and SV products are derived from the (total) energy or kinetic energy norm. For the DLM wind variance, high sensitivity has a tendency to appear around the storm region as there is generally higher ensemble variability associated with any small displacement of the strong cyclonic wind near the storm core area. Therefore, none of the above techniques for targeted observations is directly related to the motion (steering flow) of the tropical cyclone.

Theoretical work on the determination of an targeted observation strategy for improving the tropical cyclone track prediction has been lacking in literatures (a notable exception being Rohaly et al. 1998) Along with the progress in DOTSTAR, we propose a new method to determine the sensitive area for targeted observation based on the adjoint sensitivity (Zou et al. 1997; Kleist and Morgan 2005) to verify the sensitive areas with respect to the typhoon steering flow. A response function is designed to represent the steering flow at the verifying time, and to assess the adjoint sensitivity with respect to such response functions. A simple parameter is also proposed to interpret the sensitivity with clear physical meanings.

2. Methodology and experiment design

Adjoint models are powerful tools for many studies that require an estimate of sensitivity of model output with respect to input (Errico 1997). Our study utilizes a component of the MM5 (the fifth generation mesoscale model, Pennsylvania State University/National Center for Atmospheric Research) Adjoint Modeling System (Zou et al. 1997), which was used by Kleist and Morgan (2005) to investigate a snowstorm with a poor forecast. This system includes the nonlinear MM5, its tangent linear model, and corresponding dry-physics adjoint

* Corresponding author address: Chun-Chieh, Wu, Dept. of Atmospheric Sciences, National Taiwan University, No. 1, Sec. 4, Roosevelt Rd., Taipei, 106, Taiwan.
e-mail: cwu@typhoon.as.ntu.edu.tw

model. The domain for the nonlinear and adjoint model is a 60-km, 85 × 115 (latitude by longitude) horizontal grid, with 20 sigma levels in the vertical. The initial and boundary conditions are from the NCEP GFS (Global Forecasting System) global analysis (1 ° × 1 °) interpolated to the MM5 grids.

Typhoon Mindulle in 2004, one that was observed in DOTSTAR, is chosen as a test case to examine the proposed new method for targeted observations based on the adjoint sensitivity. Note that Mindulle is the sole case out of the ten DOTSTAR cases in 2004 where dropsonde data assimilated into the NCEP GFS model did not improve the track forecasts (figures not shown). The study is based on a 36-h MM5 simulation initialized at 1200 UTC 27 June 2004. The 'forward' and 'backward' integrations were executed by the MM5 forecast model and the adjoint model, respectively, as indicated in Fig. 1. The 'negative' sign in front of the time indicates the 'backward' integration (using the negative timestep) associated with the adjoint model. Figure 2 shows that the model storm moves along (but slightly faster than) the best track from the Central Weather Bureau (CWB) of Taiwan.

The work is aimed to identify the sensitive areas at the observing time (1200 UTC 27 June), which will affect the steering flow of Typhoon Mindulle at the verifying time (0000 UTC 29 June). Therefore, we define the response function(s) as the deep-layer mean wind within the verifying area. A square of 600 km by 600 km, centered around the MM5-simulated storm location (Fig. 3) at the verifying time, is used to calculate the background steering flow (Chan and Gray 1982). Two responses functions are then defined: R_1, the 850-300-hPa deep-layer area average (Wu et al. 2003) of zonal component (u), and R_2, the average of meridional component (v) of the wind vector, i.e.,

$$R_1 \equiv \frac{\int_{850hPa}^{300hPa}\int_A u \quad dxdydp}{\int_{850hPa}^{300hPa}\int_A dxdydp}, \text{and}$$

$$R_2 \equiv \frac{\int_{850hPa}^{300hPa}\int_A v \quad dxdydp}{\int_{850hPa}^{300hPa}\int_A dxdydp}. \qquad (1)$$

In other words, by averaging out the axisymmetric component of the strong cyclonic flow around the storm center, the vector of (R_1, R_2) represents the background steering flow across the storm center at the verifying time (Note that this is a wind vector, which is totally different from the kinetic energy norm described above).

In order to interpret the sensitivity with clear physical meanings, we design a unique new parameter, Adjoint-Derived Sensitivity Steering Vector (ADSSV), to identify the sensitive areas at the observing time to the steering flow at the verifying time. The ADSSV with respect to the vorticity field (ς) can be shown as

$$ADSSV \equiv \left(\frac{\partial R_1}{\partial \varsigma}, \frac{\partial R_2}{\partial \varsigma}\right), \qquad (2)$$

Where, at a given point, the magnitude of ADSSV indicates the extent of the sensitivity, and the direction of the ADSSV represents the change in the response of the steering flow with respect to a vorticity perturbation placed at that point. For example, if at a given forecast time at at one particular grid point the ADSSV vector points to the east, an increase of the vorticity at that same point at the observing time would be associated with an increase of the eastward steering of the storm at the verifying time.

3. Results

Based on Eq. (1), we first show that the background steering flow (R_1, R_2) at the verifying time in MM5 is (-6.7 m s-1, -0.8 m s-1), which is consistent with the model's westward movement of Mindulle at the verifying time (see the model's storm track in Fig. 2). In this paper, only the sensitivity products at 700 hPa are shown. In general, the results of the sensitivity patterns either at 850 or at 500 hPa are qualitatively consistent with one another.

As expected, the sensitivity (i.e., gradient) of R_1 to u (R_1/ u) at 0 h (the initial time of adjoint model) shows a response uniformly distributed over the verifying area (Fig. 3a), while there is no sensitivity of R_1 to v (R_1/ v) (Fig. 3b). To show a general sensitivity to the wind field, we combine the sensitivity of R_1 to u and the sensitivity of R_1 to v to obtain the sensitivity of R_1 to the vorticity field [$\partial R_1/\partial \varsigma$] (see the derivation in Kleist and Morgan 2005). Again, as expected, a dipolar pattern at 0 h (Fig. 3c) is found, i.e., a positive (negative) vorticity perturbation to the north (south) of the verifying area is associated with a cyclonic (anticyclonic) circulation and thus leads to an increase in R_1 (the zonal component of the mean steering flow). Meanwhile, the sensitivity of R_2 to u, v, and the vorticity field (Figs. 3d, e, and f) also reveals comparable information. In all, Figs. 3c and 3f can succinctly show the sensitivity of R_1 and R_2 to the flow field with clear physical meanings.

The evolutions of the sensitivity of R_1 and R_2 to the vorticity field are shown in Figs. 4 and 5. The sensitive areas spread from the margin of the verifying area to the outer region as the adjoint model is integrated backward in time. At –36 h (the observing time, 1200 UTC 27 June), the large gradient (and thus the high sensitivity) areas are located in the east and north of the verifying area, and the sensitivity is found to be higher in R_2 than in R_1. This means that vorticity perturbations in those large gradient (sensitive) areas at 1200 UTC 27 June will affect the steering flow of Typhoon Mindulle at 0000 UTC 29 June, particularly the meridional component of the steering flow.

As shown in Eq. (2), we can combine the result of Figs. 4 and 5 to obtain the evolution of ADSSV with respect to the vorticity field (Fig. 6). Figure 6 clearly shows that the vectors rotate around the verifying area at 0 h. As the adjoint model integrates backward in time, these vectors evolve and expand outward, with longer

vectors (i.e., higher sensitivity) mostly extending at about 800–1300 km from the north to the east of the center of verifying area.

In the above experiment, we have only demonstrated the ADSSV at one single verifying time. Nevertheless, since the tropical cyclone's final position is affected by the steering flow before and up to the verification time, it is critical to also calculate the adjoint sensitivity for different verifying times along the storm track, thus the impact of the targeted observations on the entire TC track can be better assessed. Other than performing the 36-h forward model simulation and -36-h backward adjoint integration as shown above, for the same starting (observing) time, we have also conducted the 24-h and 12-h forward and backward integrations to obtain the respective ADSSV associated with the response function (R_1, R_2) based on the respective model-predicted storm location at each verifying times. By combing all the ADSSV at -12, -24, and -36 h in one figure (e.g., see Fig. 7), we can clear identify where the sensitive regions are in affecting the steering flows at 12, 24, and 36 h, respectively, thus the regions for targeted observations to improve the typhoon track up to the verification time can be identified.

To highlight the results, the -12 (in green), -24 (in red) and - 36-h (in blue) ADSSV with respect to the vorticity field is plotted in Fig. 7, superposed with the geopotential height field at 700 hPa and the deployed locations of the dropsondes in DOTSTAR. Note that the ADSSV for different verifying times more or less collocates well with one another. Figure 7, in which the vectors in regions of large ADSSV mainly point southward, indicates the southward (northward) component of steering flow will strengthen when the vorticity in those sensitive areas is increased (decreased),. Physically, these vectors are located at the edge of the subtropical high, where, if the subtropical high strengthens (i.e., with decreased vorticity), the northward steering will increase. The results also show that the extent of the subtropical high is critical in determining Mindulle's northward turn as observed at the verifying time (figures not shown).

Besides the ADSSV with respect to the vorticity field, we also calculate the ADSSV with respect to the divergence field, which is

$$\left(\frac{\partial R_1}{\partial D}, \frac{\partial R_2}{\partial D}\right),$$

where D represents the divergence of the wind field. It is found that the sensitivity to the divergence field (figures not shown) is one order of magnitude smaller than that to the vorticity field. The above result indicates that the steering flow bears much larger sensitivity to the vorticity field than to the divergence field.

Note that the deployed locations of DOTSTAR's dropsondes are not in the region of high sensitivity in the ADSSV plot in Fig. 7. Meanwhile, the sensitive regions in Fig. 7 are quite different from those indicated by three other independent sensitivity products (figures not shown) currently used for planning the real-time targeted observations for DOTSTAR (Wu et al. 2005). Subsequent researches are needed to assess such differences and to evaluate the strength and weakness of each product.

4. Summary and prospects

In addition to various sensitivity products we have adopted in DOTSTAR, a new sensitivity measurement has been proposed based on the adjoint model. In short, by appropriately defining the response functions to represent the mean steering flow at the verifying time, we can derive its sensitivity to the flow field at the observing time to help formulate the observing strategy. In particular, a simple vector, the ADSSV with respect to the vorticity field, is proposed to clearly demonstrate the sensitivity to the storm motion. We believe that ADSSV can be applied to scientific research in many aspects and can be tested in the field project to help improve the typhoon track prediction.

Subsequent work is ongoing to consolidate this study, and will be presented in other papers.

(1) Linearity test and impact of the dry-physics adjoint model

The adjoint model is designed based on TLM, which is a linear assumptive model. As already demonstrated in Kleist and Morgan (2005), in order to validate this assumption, perturbations that evolve linearly via the TLM need to be compared with difference fields obtained from two nonlinear model forecasts to show the validity of the linear assumption.

Note that the adjoint model employed here does not include the moist physics. The moist physics is definitely critical to the development of the tropical cyclone system. Nevertheless, we believe that the tropical cyclone movement is mainly controlled by the large-scale flow field, which is likely less dependent on the moist physics. Further test on this can be conducted using the moist version of the adjoint model.

(2) Impact study

In order to validate the sensitivity derived from the adjoint modeling system, we will perturb the wind (vorticity) fields in the initial time (such as those in the area with large magnitude of ADSSV), and investigate the response of the simulated typhoon track.

(3) Other case studies

A thorough investigation of other DOTSTAR cases, such as Conson, Meari and Nock-Ten (2004), is ongoing to examine the factors affecting the motion of these storms, and to validate the proposed method on ADSSV. In particular, the ADSSV can be used to show the critical weather system affecting the storm motion, such as the impact from the approaching trough and the other storm (i.e., binary interaction).

(4) Operation in the field program

While the above task continues, we are in the process of implementing the currently designed method (using ADSSV) for real-time use in DOTSTAR, as well as for Atlantic hurricanes (in collaboration with Sim Aberson), in 2005. A longer model integration time

would then be called for because the DOTSTAR operation would require a lead time of at least 48 h. The preliminary test is showing consistent results when we run the model for up to 84 h, thus indicating the feasibility of the current system used in the DOTSTAR operation. We believe that using the method of ADSSV in DOTSTAR will shed new light on the targeted observations for tropical cyclones.

Acknowledgments. The work is supported through the National Science Council of Taiwan by Grants NSC92-2119-M-002-009-AP1 and NSC93-2119-M-002-013-AP1. The authors wish to thank Sim Aberson, Frank Marks, Sharan Majumdar, Michael Morgan, Melinda Peng and Carolyn Reynolds for their helpful suggestions and research collaborations.

References

Aberson, S. D., Targeted observations to improve operational tropical cyclone track forecast guidance, Mon. Wea. Rev., 131, 1613–1628, 2003.

Chan, J. C.-L., and W. M. Gray, Tropical cyclone movement and surrounding flow relationship. Mon. Wea. Rev., 110, 1354-1376, 1982.

Errico, R. M., What is an adjoint model? Bulletin of Amer. Meteor. Soc., 78, 2577–2591, 1997.

Gelaro, R., T. E. Rosmond, and R. Daley, Singular vector calculations with an analysis error variance metric. Mon. Wea. Rev., 130, 1166-1186, 2002.

Kleist, D. T. and M. C. Morgan, Interpretation of the structure and evolution of adjoint-derived forecast sensitivity gradients, Mon. Wea. Rev., 133, 466–484, 2005.

Majumdar, S. J., C. H. Bishop, R. Buizza and R. Gelaro, A comparison of ensemble-transform Kalman-filter targeting guidance with ECMWF and NRL total-energy singular-vector guidance, Q. J. R. Meteorol. Soc., 128, 2527–2549, 2002.

Palmer, T. N., R. Gelaro, J. Barkmeijer, and R. Buizza, Singular vectors, metrics, and adaptive observations, J. Atmos. Sci., 55, 633–653, 1998.

Pu, Z., and E. Kalnay, Targeting observations with the quasi-inverse linear and adjoint NCEP global models: Performance during FASTEX, Q. J. R. Meteorol. Soc., 125, 3329–3338, 1999.

Rohaly, G. D., R. H. Langland, and R. Gelaro, Identifying regions where the forecast of tropical cyclone tracks is most sensitive to initial condition uncertainty using adjoint methods. Preprints, 12th Conf. on Numerical Weather Prediction, Phoenix, Arizona, Amer. Meteor. Soc., 337-340, 1998.

Rosmond, T. E., A technical description of the NRL adjoint model system, NRL/MR/7532/97/7230, Naval Research Laboratory, Monterey, Calif., 93943-5502, 62pp, 1997.

Wu, C.-C., T.-S. Huang, W.-P. Huang, and K.-H. Chou, A new look at the binary interaction: Potential vorticity diagnosis of the unusual southward movement of Typhoon Bopha (2000) and its interaction with Typhoon Saomai (2000). Mon. Wea. Rev., 131, 1289-1300, 2003.

Wu, C.-C., P.-H. Lin, S. D. Aberson, T.-C. Yeh, W.-P. Huang, J.-S. Hong, G..-C. Lu, K.-C. Hsu, I-I Lin, K.-H. Chou, P.-L. Lin, and C.-H. Liu, Dropwindsonde Observations for Typhoon Surveillance near the Taiwan Region (DOTSTAR): An Overview, Bulletin of Amer. Meteor. Soc., 86, 787-790, 2005.

Zou, X., F. Vandenberghe, M. Pondeca, and Y.-H. Kuo, Introduction to adjoint techniques and the MM5 adjoint modeling system. NCAR Technical Note, NCAR/TN-435+STR, 110pp. [Available from NCAR, P.O. Box 3000, Boulder, CO 80307-3000.], 1997.Hogan, T. F., and T.E. Rosmond, 1991:"The description of the Navy Operational Global Atmospheric Prediction System's Spectral Forecast Model", Mon. Wea. Rev., 119, 1786-1815.

Majumdar, S. J., C. H. Bishop, B. J. Etherton and Z. Toth, 2002:"Adaptive sampling with the Ensemble Transform Kalman Filter. Part II: Field program implementation", Mon. Wea. Rev., 130, 1356-1369.

Surgi, N., H.-L. Pan, and S. J. Lord, 1998:"Improvement of the NCEP global model over the Tropics: An evaluation of model performance during the 1995 hurricane season", Mon. Wea. Rev., 126, 1287–1305.

Wang Y., and C.-C. Wu, 2003:"Current understanding of tropical cyclone structure and intensity changes - A review", Meteor. Atmos. Phys., 87, 257-278, DOI: 10.1007/s00703-003-0055-6.

Wu, C.-C., and Y.-H. Kuo, 1999:"Typhoons affecting Taiwan: Current understanding and future challenges", Bull. Amer. Met. Soc., 80, 67-80.

Wu, C.-C., and Coauthors, 2005a:"Dropsonde Observations for Typhoon Surveillance near the Taiwan Region (DOTSTAR): An overview", Bull. Amer. Meteor. Soc., 86, 787-790.

Wu, C. C., P. H. Lin, J. H. Chen, and K. H. Chou., 2005b:"Targeted Observations of Tropical Cyclones Based on the Adjoint-Derived Sensitivity Steering Vector", Submitted to Geophys. Res. Lett.

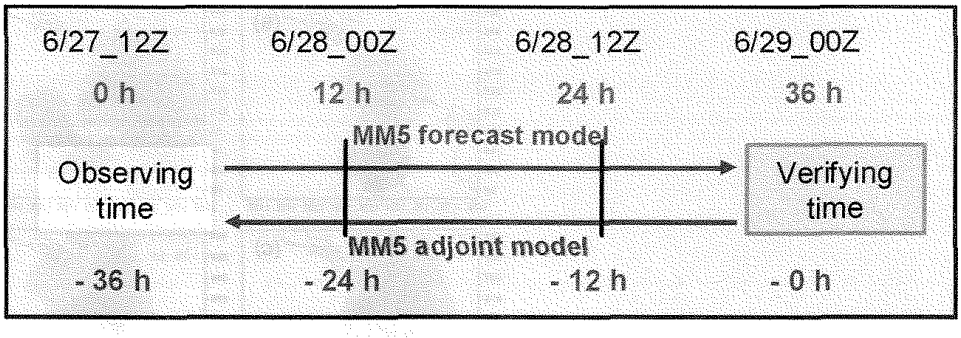

Figure 1. The design of forward and backward model integrations. The 'negative' sign in front of the time indicates the 'backward' integration (using the negative timestep) associated with the adjoint model.

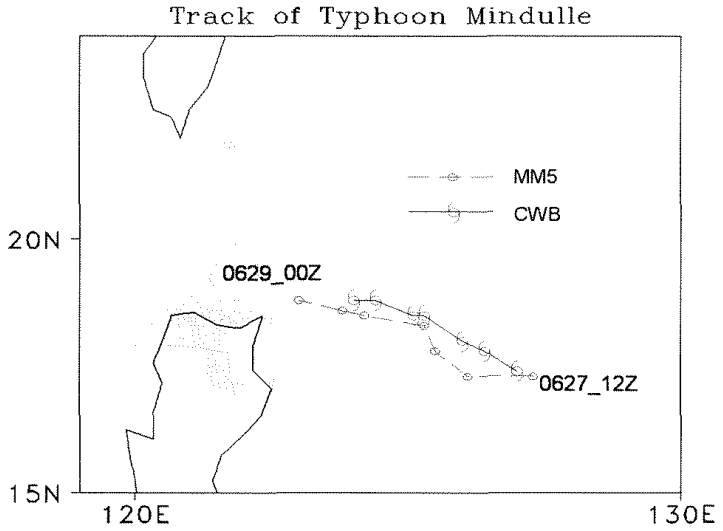

Figure 2. Tracks of Typhoon Mindulle from 1200 UTC 27 June to 0000 UTC 29 June from the MM5 forecast and the best-track analysis of CWB.

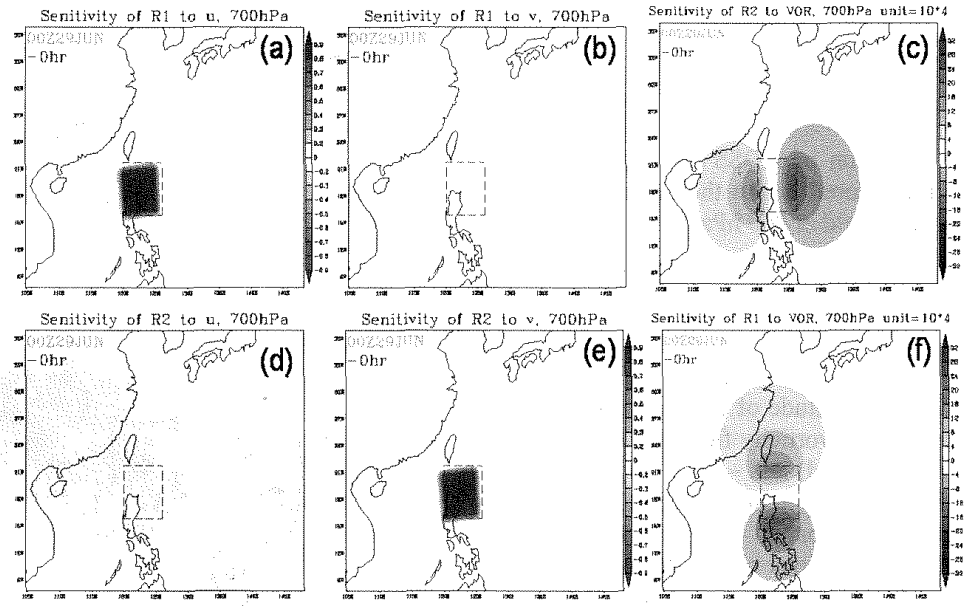

Figure 3. Sensitivity (Gradient) of R_1 to (a) u, (b) v, and (c) vorticity, and of R_2 to (d) u, (e) v, and (f) vorticity on the 700 hPa at 0 h. The magnitude of (c) and (f) is represented in the colored bar to the right, with the warm (cold) color for positive (negative) value.

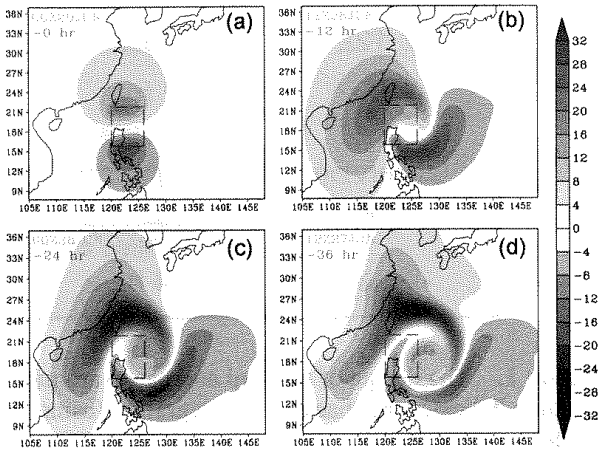

Figure 4. The evolution of sensitivity of R_1 with respect to the vorticity field at 700 hPa (magnitude in the colored bar to the right).

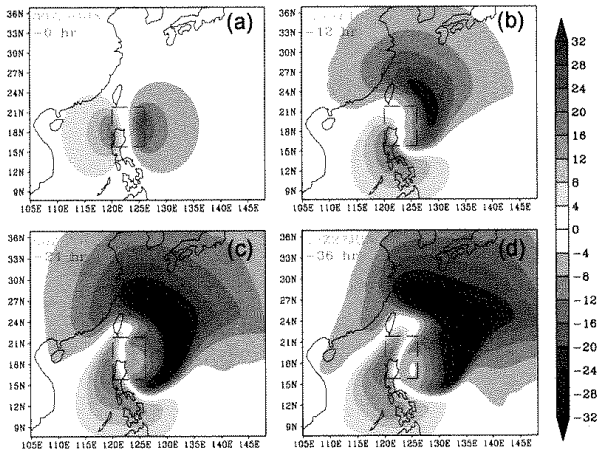

Figure 5. The evolution of sensitivity of R_2 with respect to the vorticity field at 700 hPa (magnitude in the colored bar to the right).

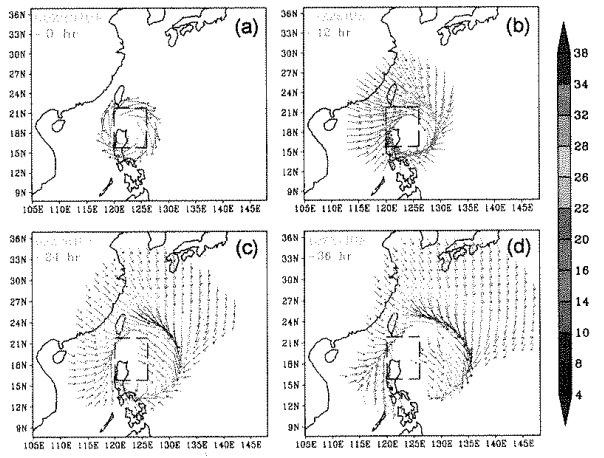

Figure 6. The evolution of ADSSV (magnitude of the vector in the colored bar to the right) with respect to the vorticity field at 700 hPa.

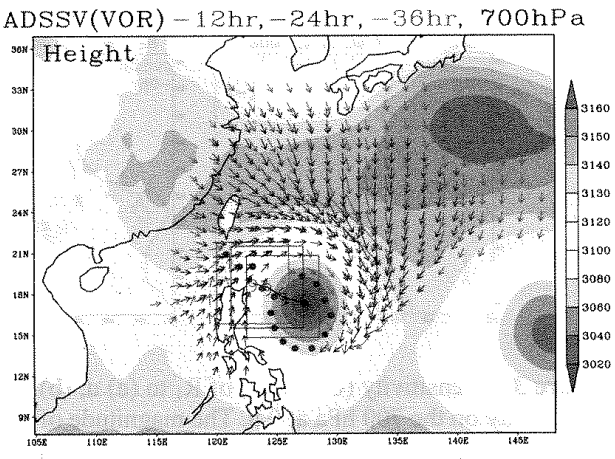

Figure 7. ADSSV (magnitude of the vector as in Fig. 6) with respect to the vorticity field at 700 hPa at -12 (in green), -24 (in red) and – 36 h (in blue), superposed with the geopotential height field (magnitude in the colored bar to the right) at 700 hPa and the deployed locations of the dropsondes in DOTSTAR (brown dots). The 36-h model-predicted track of Typhoon Mindulle is indicated with the red typhoon symbols for every 12 h.